**Journal of Sciences, Islamic Republic of Iran 14(4): 341-350 (2003)**
University of Tehran, ISSN 1016-1104

# PETROGENESIS AND ORIGIN OF THE CHENAR GRANITOID STOCK, NW OF KERMAN, IRAN: EVIDENCE OF NEOTETHYS SUBDUCTION RELATED ARC MAGMATISM

M. Arvin,[1,*] S. Dargahi,[1] and A.A. Babaei[2]

[1] *Department of Geology, College of Sciences, Shahid Bahonar University, P.O. Box 133-76175, Kerman, Islamic Republic of Iran*
[2] *Department of Biological, Geological and Environmental Sciences, Cleveland State University, Cleveland, Ohio, 44115, USA*



## Abstract

The lower to middle Miocene Chenar granitoid stock, a part of Central Iranian volcanic belt, is intruded into Eocene volcano-sedimentary complex in northwestern Kerman in south Central Iran. The Chenar granitoid stock consists mainly of coarse to medium grain granodiorite and monzogranite with subordinate tonalite and syenogranite. Alkali granites as aplitic veins and quartz dioritic dykes frequently cut through the granitoid stock. Enclaves of various types and sizes (andesitic and microgranular mafic, few meters to several centimeters wide) also occur near the margin. The granitoid rocks represent convergent margin magmas enriched in large ionic lithophile elements (LILE) such as Rb, Ba, K, Ce and depleted in high field strength elements (HFSE) such as Y, Nb and Zr. The REE patterns have relatively smooth LREE enriched chondrite normalized REE profiles with $(La/Yb)_n$ between 4.28 to 14.66. A lack of Eu anomalies along with a continuous increase in the slope of LREE profile from tonalite to syenogranite exhibit a relatively low fractionated chondrite normalized pattern [$(La/Yb)_n$] and also involvement of plagioclase in the melting processes. Small negative Eu anomaly in alkali granite is an indication of more differentiated rock type [$(La/Yb)_n$=42.78] in Chenar granitoid stock. Geochemical data, various trace element discriminant diagrams, common igneous microgranitoid enclaves, and ocean ridge granite normalized multi-element diagrams indicate that the Chenar granitoid stock has characteristics of metaluminous to slightly peraluminous, calc-alkaline, I-type granite of a volcanic arc settings and is formed in an active continental margin environment. In this model, a NE-dipping subduction zone of Neotethys could have accounted for the arc volcanism of the Central Iran where felsic, Andean-type magmatic arc volcanics and plutonics were formed. As a result of subduction mafic arc magmas with significant fluids were produced following the dehydration of oceanic crust and partial melting of mantle wedge which in turn provoke partial melting of considerably metasomatised and enriched subcontinental lithosphere, leading to generation of siliceous magma. Its low-pressure crystal fractionation gave rise to generation of hydrous calc-alkaline magmas, represented in part by Chenar granitoid stock.

**Keywords:** Chenar stock; Volcanic arc granitoid; I-type; Neotethys; Central Iran

## 1. Introduction

The lower Miocene Chenar granitoid stock [9] is part of Dehaj- Sarduiyeh volcano-sedimentary belt, which forms a distinctive part of Central Iranian volcanic belt or the "Urmiah-Dukhtar belt" of Schroeder [23] (Fig. 1). This belt forms a characteristic, linear, intrusive-extrusive complex (~150 km width) which extends for

* *E-mail: arvin@mail.uk.ac.ir*

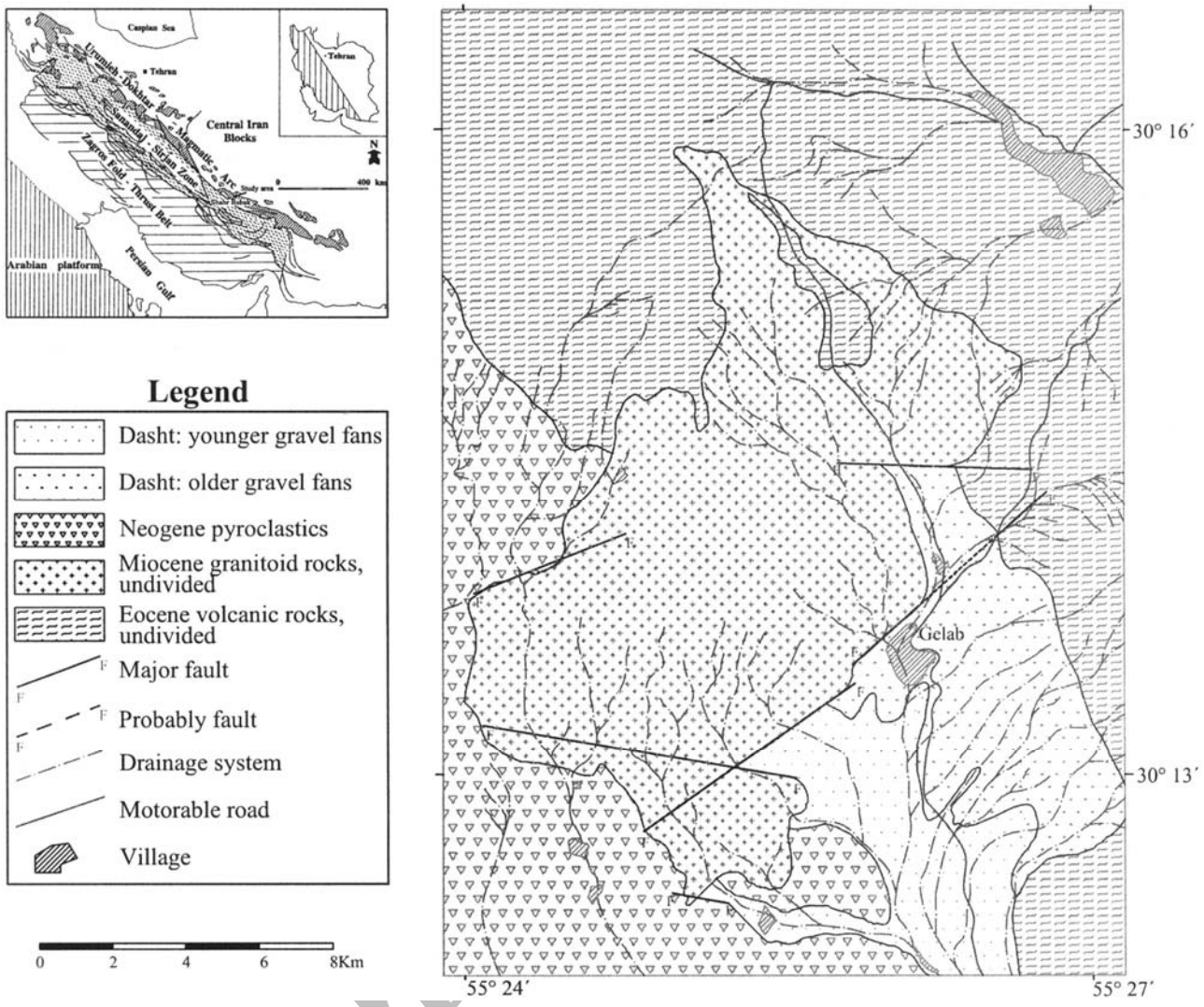


**Figure 1.** Location and geological map of the Chenar granitoid stock.

1700 km parallel to the entire length of the Zagros orogenic belt. It consists of various lithologic units such as small to large plutonic bodies of granite, diorite, gabbro, widely distributed basaltic lava flows, trachybasalts (locally shoshonitic), andesite, dacite, trachyte, ignimbrite and pyroclastics (mostly tuff and agglomerate). The oldest known pluton in this assemblage is calc-alkaline intrusive rocks of Precambrian age exposed in the southeastern margin of Central Iran [3]. The youngest rocks (mainly lava flows and pyroclastics) belong to Quaternary Pliocene volcanic cones of alkaline and calc-alkaline composition.

The purpose of this paper is to present petrographical, geochemical and petrogenetic characteristics of the Chenar granitoid stock and its role in the Oligocene-Miocene plutonism subduction related terraines in the Kerman region.

## 2. Field Relationships

The Chenar granitoid rocks, located 230 km northwest of Kerman in southern Iran (Fig. 1), form a stock-like intrusive mass mostly of acidic composition. In the eastern part of the study area, the granitoid rocks intruded the Eocene volcano-sedimentary complex, which consists of andesite, trachyandesite, trachybasalt, andesitic basalt, trachyte, tuff and volcano-clastic, and to the west they are covered by Pliocene volcano-clastic rocks of Masahim volcano.

The Chenar granitoid rocks consist mainly of granodiorite and monzogranite, with subordinate tonalite and syenogranite (nomenclature follows

LeMaitre, [15]). Their magmatic contact with Eocene volcano-sedimentary complex is marked by albite-epidote to hornblende hornfels facies and granitic apophyses. The granitoid stock frequently cut by alkali granite as aplitic veins and quartz dioritic dykes. Enclaves of various types and sizes (centimeters to meters) occur near the margin. The enclaves can be divided into two groups: xenolithic enclaves (andesitic in composition) and microgranular mafic enclaves (dioritic, quartz dioritic, monzodioritic, quartz monzo-dioritic, quartz monzonitic and monzonitic in composition). The distribution of enclaves is not even in the area. In some section they form individual masses, while in other areas they form swarms. The swarms are mostly microgranular mafic enclaves and they exist as planar and nonplanar dyke shape, small raft, vortex and folded lens-shape swarms.

The Chenar granitoid rocks are cut by different types of dykes of different sizes and orientations. These dykes consist of aplitic to pegmatitic alkali granites (0.01-1.5 m wide), microgranular dykes (0.1-4 m wide) which are similar to mafic enclaves in composition and basic to intermediate aphanitic dykes (0.5-0.8 m wide).

The granitoid rocks also show evidence of hydrothermal and late magmatic activities, marked by argillation of K-feldspars, sericitization and saussuritization of plagioclase, uralitization of clinopyroxenes and tourmalinization. Sulfide minerals (mainly pyrite and to lesser extent chalcopyrite), azurite and malachite often occur along the joint systems.

## 3. Petrography

Rocks of the Chenar granitoid stock are coarse to medium grained and are hypidiomorphic inequigranular. They commonly contain quartz (<10-50%), plagioclase (<10-75%), alkali-feldspar (0-75%) and ferromagnesian minerals (5-25%). Fine (mm-size) accessory apatite and zircon are intergranular and form inclusions in amphibole and biotite. Other accessory minerals are titanite (as much as 4 mm long) and magnetite. The rocks are variably strained; typically with weak subgrain development in quartz grains marked with undulatory extinction and lesser, fish like biotite and bent or broken plagioclase. Quartz grains are generally clustered between the feldspars with micrographic and occasionally granophyric intergrowth. Often quartz phenocryts with sutured boundaries have inclusions of the other granitoid minerals. Plagioclase varies from oligoclase to labradorite with some crystals exhibiting oscillatory zoning and sieve texture and are affected by saussuritization. Myrmekitic intergrowths and micro-perthitic textures are also common. Alkali feldspar (orthoclase) occurs as phenocrysts with sutured boundaries, perthitic crystals and intergrowth with quartz in the matrix. The orthoclase is also affected by sericitization and kaolinitization processes. Ferro-magnesian minerals includes biotite (altered to chlorite, titanite and iron oxides), hornblende (altered to chlorite, calcite and epidote), and clinopyroxene (diopside-augite, occasionally resorbed and overgrowth by hornblende) which is often uralitized. In the uralitized clinopyroxene, magnetite is formed along the cleavage traces, which may attest to reduction of lateral pressure during on the ascending magma, which resulted in the instability of diopside [19]. The absence of primary perthite, formation of plagioclase and alkali feldspar as a separate phases, and micrographic and myrmekitic textures along with deutric alteration suggest the crystallization of the Chenar granitoid rocks in a sub-solvus condition at relatively high $P_{H2O}$ (>5 kb).

## 4. Enclaves

Mafic microgranular enclaves in general consist of phenocrysts of plagioclase + alkali feldspar + quartz + hornblende in a groundmass of plagioclase, quartz, biotite, hornblende and opaque minerals. Plagioclase phenocryts of andesine to bytownite, display oscillatory zoning and seive textures. Alkali feldspar and quartz occur as oikocrysts near the contact with their host granitoid rocks. Some of these feldspars and quartz grains have formed in the host rock, and the others with poikilitic texture remain in enclaves surround the other crystals in the matrix. This places the root of oikocrysts in granitoid rocks (*i.e.*, porphyroblast origin). Thus the parent magma of mafic enclaves could have been diorite that has been contaminated later with a host acidic magma. This change of composition of enclaves into monzodiorite and monzonite and their enrichment in alkali feldspars depends on the rate of contamination.

Apatite is seldom present as equant grains. Other accessory minerals are subhedral to interstitial titanite and zircon as subhedral granular grains. The presence of igneous enclaves within granite indicates that more mafic magmas may have been involved for the formation of the origin of granitic magma [25].

Enclaves of host Eocene volcanic rocks (andesite and andestic basalt) also occur in granitoid rocks near the margin.

## 5. Geochemistry

Major and trace element abundances (Table 1) were determined for twenty-eight carefully selected fresh samples by X-ray fluorescence using a Phillips 1220-C

**Table 1.** Major, trace and rare earth element analyses of the Chenar granitoid stock

| **Sample** | **PD4** | **QRB6** | **AG3** | **QCL12** | **BG6** | **QDL13** | **CL9** | **DL30** | **RB3** | **AG19** | **AG8** | **BG11** | **BG7** | **CL21** |
|---|---|---|---|---|---|---|---|---|---|---|---|---|---|---|
| **Rock type** | **Tn** | **Tn** | **Gd** | **Gd** | **Gd** | **Gd** | **Gd** | **Gd** | **Gd** | **Mg** | **Mg** | **Mg** | **Mg** | **Mg** |
| wt% | | | | | | | | | | | | | | |
| $SiO_2$ | 61.34 | 61.33 | 65.10 | 67.38 | 66.26 | 64.35 | 67.22 | 68.28 | 68.42 | 63.29 | 68.02 | 71.49 | 66.12 | 67.06 |
| $TiO_2$ | 0.89 | 0.66 | 0.67 | 0.48 | 0.49 | 0.46 | 0.56 | 0.53 | 0.52 | 0.61 | 0.36 | 0.26 | 0.59 | 0.79 |
| $Al_2O_3$ | 18.16 | 15.93 | 17.22 | 14.83 | 16.81 | 15.92 | 16.41 | 16.50 | 16.43 | 17.39 | 16.30 | 15.85 | 17.08 | 16.04 |
| FeO | 4.82 | 6.27 | 4.42 | 3.66 | 3.54 | 4.14 | 3.63 | 3.86 | 4.95 | 4.30 | 2.94 | 2.56 | 4.15 | 4.95 |
| MnO | 0.17 | 0.14 | 0.10 | 0.10 | 0.09 | 0.10 | 0.12 | 0.10 | 0.08 | 0.11 | 0.07 | 0.06 | 0.09 | 0.10 |
| MgO | 3.39 | 2.92 | 2.05 | 1.98 | 1.67 | 2.45 | 2.09 | 1.67 | 1.11 | 2.59 | 1.30 | 1.28 | 2.31 | 2.12 |
| CaO | 5.67 | 7.88 | 4.73 | 5.28 | 4.04 | 5.32 | 5.14 | 4.36 | 4.28 | 5.16 | 3.41 | 2.59 | 4.20 | 4.07 |
| $Na_2O$ | 3.64 | 2.29 | 3.26 | 2.13 | 4.41 | 2.66 | 3.08 | 2.96 | 2.75 | 4.44 | 3.77 | 3.20 | 3.47 | 2.95 |
| $K_2O$ | 1.73 | 1.74 | 2.29 | 3.34 | 2.50 | 3.74 | 1.92 | 1.93 | 1.54 | 2.04 | 3.94 | 2.53 | 2.10 | 1.97 |
| $P_2O_5$ | 0.01 | 0.21 | 0.08 | 0.18 | 0.07 | 0.18 | 0.06 | 0.05 | 0.01 | 0.06 | 0.07 | 0.07 | 0.08 | 0.11 |
| LOI | 0.32 | 0.55 | 0.13 | 0.44 | 0.11 | 0.47 | 0.14 | 0.15 | 0.24 | 0.05 | 0.03 | 0.10 | 0.07 | 0.90 |
| Total | 100.14 | 99.93 | 100.05 | 99.79 | 99.99 | 99.79 | 100.37 | 100.39 | 100.33 | 100.04 | 100.21 | 99.99 | 100.26 | 101.06 |
| ppm | | | | | | | | | | | | | | |
| V | 220 | 97 | 68 | 65 | 97 | 27 | 48 | 25 | | | | | | |
| Cr | 44 | 18 | 32 | 31 | 72 | 13 | 44 | 14 | | | | | | |
| Ni | 23 | 8 | 11 | 14 | * | 15 | * | 17 | | | | | | |
| Cu | 134 | 19 | 61 | 2 | 58 | 23 | 23 | * | | | | | | |
| Rb | 32 | 50 | 108 | 111 | 139 | 186 | 171 | 257 | | | | | | |
| Sr | 417 | 435 | 522 | 552 | 558 | 602 | 354 | 542 | | | | | | |
| Y | 20 | 16 | 20 | 20 | 18 | 21 | 12 | 21 | | | | | | |
| Zr | 97 | 105 | 127 | 134 | 169 | 119 | 117 | 115 | | | | | | |
| Nb | 4 | 2 | 6 | 7 | 7 | 4 | 9 | 5 | | | | | | |
| Ba | 446 | 400 | 825 | 793 | 1110 | 855 | 721 | 876 | | | | | | |
| Pb | 30 | 8 | 32 | 31 | 20 | 20 | 28 | 17 | | | | | | |
| Th | 4.7 | 2 | 6 | 6 | 16.9 | 13 | 24.3 | 16 | | | | | | |
| U | 1.2 | 1 | 7 | 4 | 5.2 | 5 | 3.1 | 4 | | | | | | |
| Hf | 2.6 | | | | 4.4 | | 3.4 | | | | | | | |
| Ta | 0.2 | | | | 0.6 | | 0.7 | | | | | | | |
| Tl | 0.2 | | | | 0.7 | | 1.1 | | | | | | | |
| La | 11.8 | | | | 27.5 | | 27.2 | | | | | | | |
| Ce | 24.4 | | | | 48.8 | | 42.7 | | | | | | | |
| Pr | 3.01 | | | | 5.32 | | 4.11 | | | | | | | |
| Nd | 12.8 | | | | 20 | | 13.9 | | | | | | | |
| Sm | 3.2 | | | | 3.8 | | 2.5 | | | | | | | |
| Eu | 0.99 | | | | 1.1 | | 0.68 | | | | | | | |
| Gd | 3.1 | | | | 3.1 | | 1.8 | | | | | | | |
| Tb | 0.6 | | | | 0.5 | | 0.3 | | | | | | | |
| Dy | 3.3 | | | | 3 | | 1.9 | | | | | | | |
| Ho | 0.7 | | | | 0.6 | | 0.4 | | | | | | | |
| Er | 2 | | | | 1.8 | | 1.2 | | | | | | | |
| Tm | 0.32 | | | | 0.28 | | 0.21 | | | | | | | |
| Yb | 1.9 | | | | 1.8 | | 1.4 | | | | | | | |
| Lu | 0.31 | | | | 0.29 | | 0.23 | | | | | | | |

* Not analyzed. Tn, tonalite; Gd, granodiorite; Mg, monzogranite; Sg, syenogranite; Ag, alkali granite; Di (dy), diorite (dyke); Di (en), diorite (enclave); Qd (en); quartz diorite (enclave); Qd (dy), quartz diorite (dyke)

**Table 1.** Continue

| Sample | DL28 | QAG13 | NB9 | QBG1 | DL1 | QDL1 | BG61 | QBG61 | QBG81 | CL111 | CL112 | QCL112 | DL81 | QDL101 |
|---|---|---|---|---|---|---|---|---|---|---|---|---|---|---|
| Rock type | Mg | Mg | Mg | Mg | Sg | Sg | Ag | Ag | Ag | Qd(dy) | Di(dy) | Di(dy) | Di(en) | Qd(en) |
| wt% | | | | | | | | | | | | | | |
| $SiO_2$ | 67.55 | 65.64 | 68.30 | 66.71 | 72.21 | 69.37 | 73.43 | 77.35 | 74.79 | 52.83 | 47.81 | 50.81 | 52.38 | 57.12 |
| $TiO_2$ | 0.64 | 0.44 | 0.58 | 0.44 | 0.19 | 0.25 | 0.10 | 0.10 | 0.15 | 0.88 | 0.78 | 0.57 | 0.86 | 0.76 |
| $Al_2O_3$ | 16.59 | 15.78 | 16.67 | 15.42 | 16.01 | 15.33 | 14.26 | 12.36 | 13.69 | 16.13 | 15.14 | 15.24 | 18.90 | 16.35 |
| FeO | 3.86 | 3.92 | 4.02 | 3.51 | 1.90 | 1.54 | 1.88 | 0.74 | 1.22 | 10.00 | 13.08 | 11.80 | 8.70 | 7.19 |
| MnO | 0.12 | 0.09 | 0.08 | 0.08 | 0.04 | 0.04 | 0.06 | 0.01 | 0.02 | 0.19 | 0.24 | 0.19 | 0.20 | 0.18 |
| MgO | 1.91 | 1.94 | 1.46 | 1.92 | 0.92 | 0.61 | 0.64 | 0.02 | 0.26 | 7.29 | 9.21 | 7.14 | 4.27 | 3.27 |
| CaO | 4.50 | 5.11 | 4.22 | 4.74 | 1.99 | 2.25 | 1.11 | 1.21 | 1.37 | 6.78 | 9.96 | 8.89 | 8.15 | 7.47 |
| $Na_2O$ | 2.94 | 2.45 | 3.24 | 2.28 | 3.00 | 2.35 | 4.37 | 2.34 | 2.72 | 3.79 | 2.44 | 1.74 | 4.17 | 3.07 |
| $K_2O$ | 2.06 | 3.66 | 1.57 | 4.01 | 3.98 | 7.74 | 4.11 | 5.20 | 5.14 | 1.38 | 0.66 | 1.07 | 1.59 | 2.49 |
| $P_2O_5$ | 0.06 | 0.18 | 0.06 | 0.19 | 0.01 | 0.08 | 0.01 | 0.01 | 0.03 | 0.19 | 0.12 | 0.11 | 0.17 | 0.42 |
| LOI | 0.08 | 0.52 | 0.11 | 0.41 | 0.11 | 0.34 | 0.04 | 0.49 | 0.40 | 0.87 | 0.57 | 2.34 | 0.45 | 1.23 |
| Total | 100.31 | 99.73 | 100.31 | 99.71 | 00.36 | 99.90 | 100.01 | 99.83 | 99.79 | 100.33 | 100.01 | 99.90 | 99.84 | 99.56 |
| ppm | | | | | | | | | | | | | | |
| V | | 62 | | 66 | 42 | 37 | 12 | 22 | 27 | 113 | * | 147 | 106 | 126 |
| Cr | | 30 | | 42 | 75 | 42 | 65 | 35 | 86 | 65 | * | 162 | 26 | 46 |
| Ni | | 17 | | 9 | * | 11 | * | 6 | 4 | 135 | 11 | 87 | 26 | 21 |
| Cu | | 23 | | 609 | 78 | 61 | 29 | 8 | 28 | 77 | 58 | 5 | 248 | 91 |
| Rb | | 107 | | 111 | 226 | 193 | 210 | 185 | 155 | 76 | * | 80 | 66 | 98 |
| Sr | | 514 | | 525 | 537 | 494 | 74 | 76 | 306 | 638 | 866 | 691 | 630 | 423 |
| Y | | 20 | | 19 | 8 | 23 | 14 | 24 | 21 | 40 | 24 | 15 | 29 | 20 |
| Zr | | 136 | | 132 | 149 | 130 | 94 | 87 | 96 | 161 | 101 | 63 | 163 | 120 |
| Nb | | 6 | | 4 | 5 | 4 | 15 | 7 | 3 | 8 | 5 | 2 | 10 | 6 |
| Ba | | 729 | | 827 | 2960 | 2183 | 131 | 49 | 705 | 628 | 338 | 192 | 772 | 520 |
| Pb | | 21 | | 30 | 27 | 36 | 37 | 49 | 32 | 18 | 16 | 18 | 24 | 30 |
| Th | | 10 | | 4 | 34.8 | 15 | 51.6 | 41 | 24 | 12 | 7 | 2 | 12 | 5 |
| U | | 1 | | 1 | 9.9 | 9 | 12 | 8 | 6 | 3 | * | 1 | 4 | 1 |
| Hf | | | | | 4.6 | | 4.1 | | | | | | | |
| Ta | | | | | 0.5 | | 1.5 | | | | | | | |
| Tl | | | | | 1.1 | | 0.7 | | | | | | | |
| La | | | | | 56.1 | | 38.5 | | | | | | | |
| Ce | | | | | 89 | | 62.9 | | | | | | | |
| Pr | | | | | 8 | | 5.87 | | | | | | | |
| Nd | | | | | 24.5 | | 18.6 | | | | | | | |
| Sm | | | | | 2.9 | | 2.8 | | | | | | | |
| Eu | | | | | 0.88 | | 0.35 | | | | | | | |
| Gd | | | | | 1.4 | | 1.8 | | | | | | | |
| Tb | | | | | 0.2 | | 0.4 | | | | | | | |
| Dy | | | | | 1.3 | | 2 | | | | | | | |
| Ho | | | | | 0.2 | | 0.4 | | | | | | | |
| Er | | | | | 0.8 | | 1.4 | | | | | | | |
| Tm | | | | | 0.11 | | 0.26 | | | | | | | |
| Yb | | | | | 0.9 | | 1.8 | | | | | | | |
| Lu | | | | | 0.16 | | 0.31 | | | | | | | |

computerized spectrometer at Geological Survey of Iran. In addition, samples of major rock units in the Chenar granitoid stock were analyzed for rare-earth element (Table 1) by ICP-MS in Acta Laboratory in Canada. Major element oxides $Al_2O_3$, FeO, $TiO_2$, CaO, MgO and MnO all have a negative correlation with silica (Fig. 2).

Trace element distributions are erratic, with only two elements showing any significant trend. Vanadium has a negative correlation and Nb has a positive correlation with $SiO_2$, and both are consistent with the general trend of a differentiation granitic magma.

The Chenar granitoid samples define a typical calc-alkaline trend on an AFM diagram (Fig. 3a), although on $K_2O$ *vs.* $SiO_2$ diagram, some tendency toward high-k calc-alkaline trend is obvious (Fig. 3b) which may point to the depth of subduction. Classification by the aluminum saturation index (ASI) of Zen [28] indicates that most of the samples are metaluminous and some are slightly peraluminous (*i.e.* Al index<1.1) (Fig. 3c). The peraluminous nature of samples may be the result of differentiation of hornblende [28] or heterogeneity of the water content in the protholith [26]. However, the overall mineralogy of the granitoid rocks which include clinopyroxene, hornblende, biotite, magnetite, apatite, zircon, titanite, allanite, and epidote strongly suggest a metaluminous source.

The major and trace elements have been used for classification of similar rocks, determination of their source rocks, and interpretation of their tectonic settings [5,11,13,16,17,20,21].

The discrimination between ocean ridge granites (ORG), volcanic arc granites (VAG), within plate granites (WPG) and collision granites (COLG) have been purposed by Pearce *et al*. [21] using Nb, Y, Ta, Yb and Rb trace element data. Pearce [20] explained the importance of Rb *vs*. (Nb+Y) for determining the source for the granites and their geological background. On the Nb *vs*. Y and Rb *vs*. (Nb+Y) diagrams (Figs. 4a, b), the Chenar granitoid rocks plot within the volcanic arc granite (VAG) field with slight affinity toward syn-COLG. This could be due to crustal contamination [21]. The VAG setting and pre-plate collision nature of the Chenar granitoid rocks are further evident from Ta-Hf-Rb diagram [11], and Y *vs*. Zr diagram [17] (Figs. 5a,b).

The Nb and Y concentrations in volcanic arc granites usually represent the type of source. Pearce [20] suggested that the source for the volcanic arc granites could be a depleted asthenosphere that juxtaposes against a crustal counterpart during a subduction process. The lack of any increase in Nb+Y (Table 1) is a sign of relatively low degree of fractional crystallization in volcanic arc granites.

The studies of similar plutons (Pearce *et al*., [21], for example) suggest that the granitoid stocks (such as Chenar) enriched in large ionic lithophile elements (LILE) relative to high field strength elements (HFSE) (Fig. 6) are typical of continental margin. Enrichment of $K_2O$, Rb, Th, Ce and negative Nb anomaly in Chenar granitoid stock are compatible with the concentration of these elements in continental arc suites.

The REE patterns of the granitoid stocks must reflect the residual mineral assemblages of their source region [26]. The whole rock REE analyses for five representative rock types from the Chenar granitoid rocks are included in Table 1. Most samples have a relatively smooth, LREE enriched, chondrite-normalized REE profiles (Fig. 7) with $(La/Yb)_n$ between 4.28 to 14.66. A lack of Eu anomalies in four of the samples (tonalite, monzogranite, granodiorite, syenogranite) along with a continuous increase in the slope of LREE profile from tonalite to syenogranite, clearly exhibit a relatively low fractionated chondrite normalized REE patterns [$(La/Yb)_n$)]. Cullers and Graf [7] showed that granitic rocks containing no Eu anomalies, low to moderate REE contents and variable LREE/HREE ratios require little or no residual plagioclase in the source. This clearly shows that plagioclase was involved in the melting processes. This is in line with experimental data that suggest most I-type granites formed by hydration melting at temperatures greater than about 850°C [24]. However, small negative Eu anomaly in alkali granite is an indication of a more differentiated rock type [$(La/Yb)_n$=42.78] in the Chenar granitoid stock.

## 6. Discussion and Conclusion

The Dehaj-Sarduiyeh volcanic belt, which includes the lower Miocene granitic rocks of the Chenar, is part of Central Iranian volcanic belt. This belt is the subject of considerable controversy concerning the nature and dating of the final closure of the Neotethys ocean and the Arabian- Central Iranian continental collision process. The existence of the Central Iranian volcanic belt has been explained by many as the result of a northeast dipping subduction along the Main Zagros reverse fault, at an Andean- type magmatic arc along the active continental margin of Central Iran. Berberian *et al*. [4] believed that the latest Andean type magmatic activity took place during the Oligocene-Miocene that was followed by the magmatic arc migrate inland. Other studies suggest that the Eocene volcanic activities in Central Iran began by the opening up of the basins and creation of a horst-graben system [1,2,6,8,10]. This aspect suggests that the contamination of a basaltic

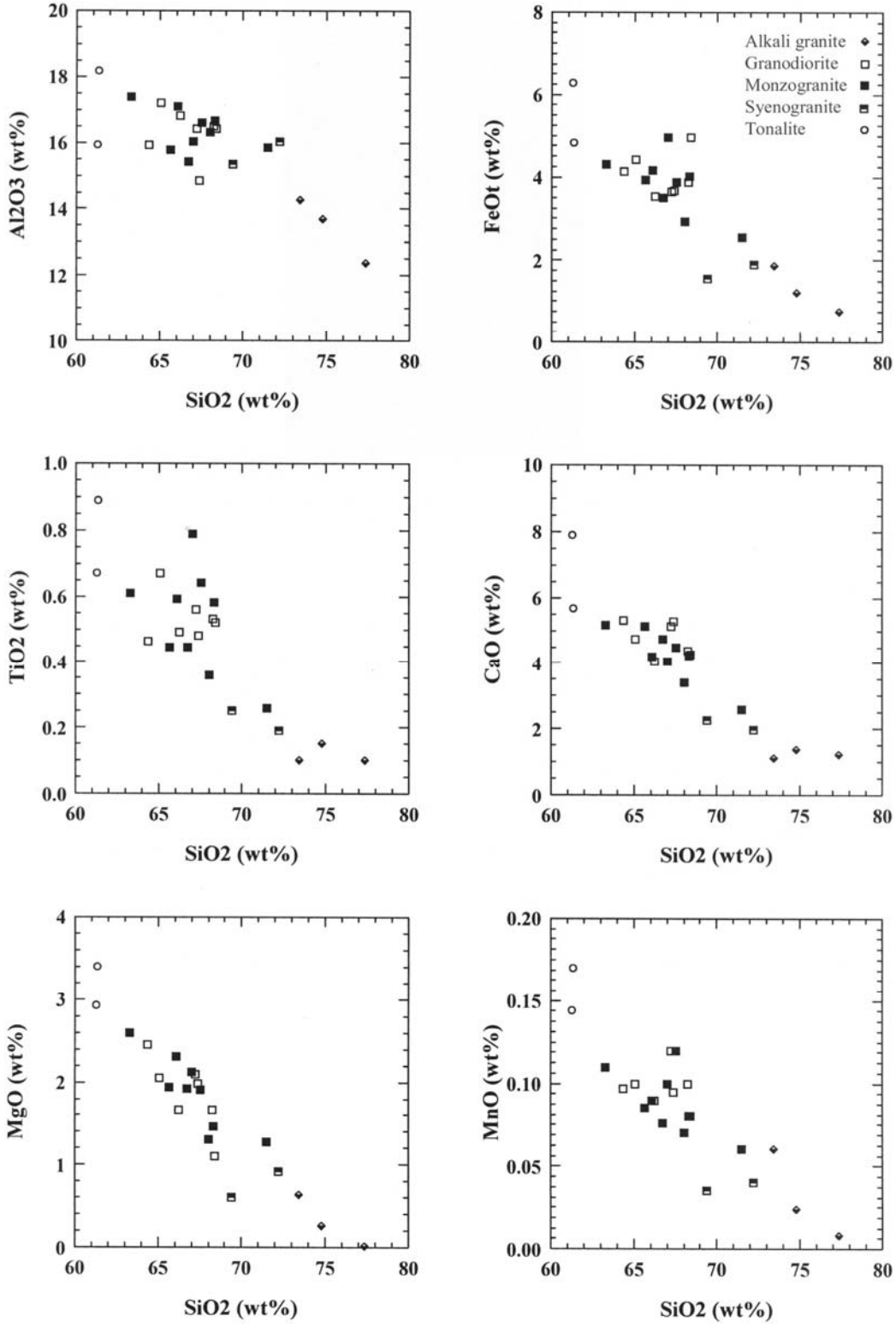


**Figure 2.** Selected major element oxide variation plotted *vs.* $SiO_2$ content.

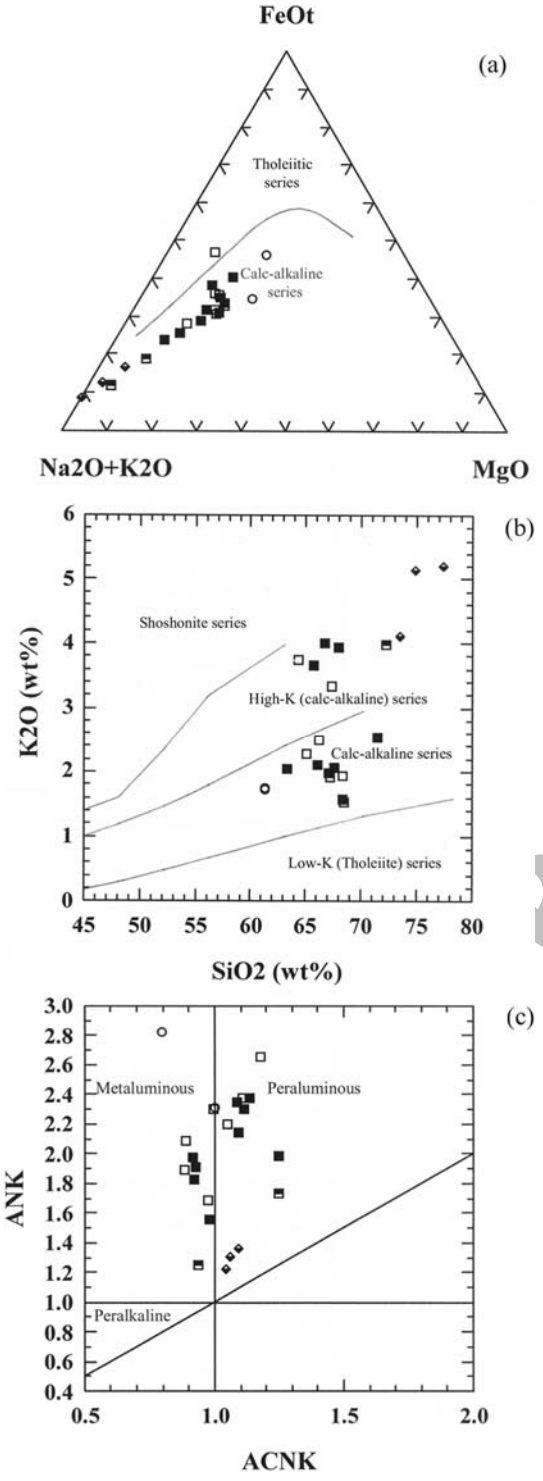


**Figure 3.** AFM diagram showing chemical trend for the Chenar granitoid rocks. Dot line: boundary line of Kuno [14], (b), $SiO_2$ *vs.* $K_2O$ classification diagram (after [15]) for the Chenar granitoid stock and (c) plot of A/NK *vs.* A/CNK [A/NK=molar ratio of $Al_2O_3/(Na_2O+K_2O)$; A/CNK = molar ratio of $Al_2O_3/(CaO+Na_2O+K_2O)$] for the Chenar granitoid stock. Symbols as in Figure 2.

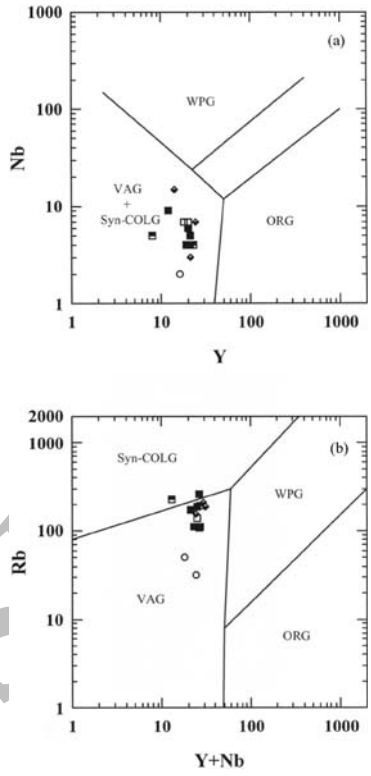


**Figure 4.** Trace element discrimination diagrams for the Chenar granitoid rocks [20, 21]. VAG=volcanic arc granites, ORG=ocean ridge granites, WPG=within-plate granites, syn-COLG=syn-collision granites, and post-COLG=post-collision granites. Symbols as in Figure 2.

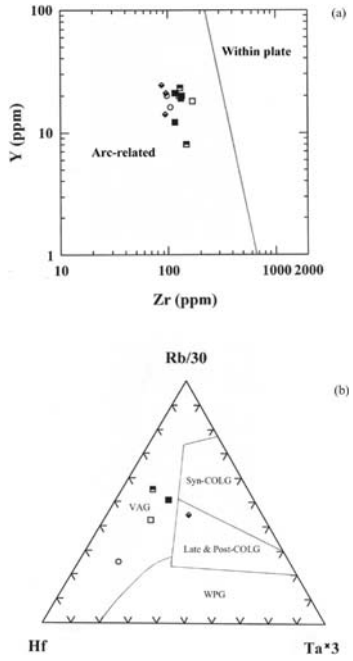


**Figure 5.** Zr *vs.* Y [17] and Hf-Rb-Ta [11] discrimination diagrams for the Chenar granitoid rocks. Symbols as in Figure 2.

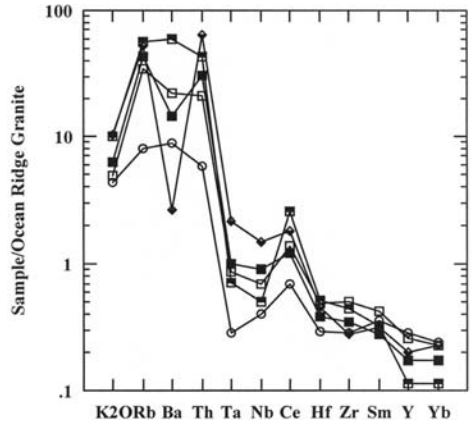


**Figure 6.** Ocean ridge granite (ORG) normalized geochemical patterns for the Chenar granitoid stock (normalization factors from Pearce *et al*., [21]). Symbols as in Figure 2.

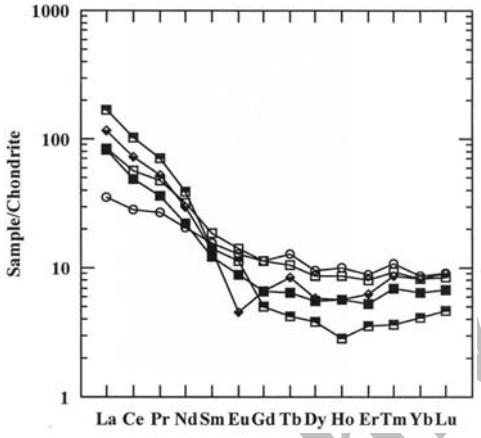


**Figure 7.** Chondrite-normalized REE plots of the Chenar granitoid rocks. Normalizing values used are from Nakamura [18]. Symbols as in Figure 2.

magma by a bulky, palingenetic acid magma is the explanation for the few volcanic rocks with calc-alkaline trends in the Central Iranian volcanic belt.

The Chenar granitoid stock consists mainly of granodiorite and monzogranite with subordinate tonalite and syenogranite (an evidence of an in situ differentiation), and all of them contain hornblende and to certain extent mafic enclaves. Alkali granite (as aplitic vein) and quartz dioritic rocks also frequently cut through the granitoid stock. Metaluminous composition, strong mineralogical (magnetite and titanite bearing) and geochemical (A/CNK<1.1) characteristics, amphibole-bearing minerals, and common igneous microgranitoid enclaves indicate plutonic rocks of the Chenar have affinity with I-type granite. On the various trace element tectono-magmatic discrimination diagrams [17,20,21], the Chenar granitoids are classified as continental arc type. In this context, a NE dipping subduction zone could have accounted for arc volcanism established over the Central Iranian microcontinental mass along which felsic, Andean- type arc volcanics and plutonics were formed [4,12]. As a result of this subduction mafic arc magmas with significant fluids were produced following the dehydration of oceanic crust and partial melting of mantle wedge which in turn provoke partial melting in the subcontinental lithosphere which is considerably metasomatised and enriched [22,27]. This led to generation of siliceous magma. Low-pressure crystal fractionation of such magma gave rise to generation of hydrous calc-alkaline magmas, represented in part by the Chenar granitoid stock. Deep-seated crustal melting, and some mantle-derive mafic magma hybridized with crustal melts formed intermediate mafic melt that consequently formed the mafic enclaves and dykes. All these suggest that mixing of mafic and granitic magmas was the main mechanism for the formation of mafic enclaves and dykes in the Chenar granitoid stock.

## Acknowledgements

The authors would like to thank anonymous reviewers for their critical and constructive comments on the manuscript.

## References

1. Amidi S.M. Contribution a l' etude stratigraphique, petrologique et petrochemique des roches magmatiques de la region de Natanz-Nain-Surk (Iran Central). [Dissertation], Grenoble, 316 pp. (1975).
2. Amidi S.M., Emami M.H., and Michel R. Alkaline character of Eocene volcanism in the middle part of Central Iran and its geodynamic situation. *Geol. Rundschau*, **73**: 917-932 (1984).
3. Berberian F. and Berberian M. Tectono-plutonic episods in Iran. Geodynamic Series 3, working group 6, American Geophysical Union, 5-32 (1981).
4. Berberian F., Muir I.D., Pankhurst R.J., and Berberian M. Late Cretaceous and Early Miocene Anden-type plutonic activity in northern Makran and Central Iran. *J. Geol. Soc. London*, **139**: 605-614 (1982).
5. Bowden P., Batchelor R.A., Chappell B.W., Didier J., and Lameyre J. Petrological, geochemical and source criteria for the classification of granitic rocks: a discussion. *Physics of the Earth and Planetary Interiors*, **35**: 1-11 (1984).
6. Caillat C., Dehlavi P., and Martel-Jantin B.C. Geologie de la region de Saveh (Iran) contribution a l'etude du volcanism etdu plutonism tertiaires de la zone de l' Iran

Central. [Dissertation], Grenoble, 325 p. (1978).
7. Cullers R.L. and Graf J.L. Rare earth elements in igneous rocks of the continental crust: intermediate and siliceous rocks- or petrogensis. In: Henderson, P. (Ed.), *Rare Earth Element Geochemistry*. Elsevier, 510 pp. (1989).
8. Didon J. and Gemain Y.M. La Sabalan volcan plio-Quarternaire de l'Azerbaidjan oriental (Iran). [Dissertation], Grenoble, 304 pp. (1976).
9. Dimitrijevic M.D. Geology of Kerman Region. G.S.A., Rep. No. Yu/52., 334 pp. (1973).
10. Emami M.H. Geologie de la region de Qom-Aran (Iran). Contribution a 1'etude dynamique et geochemique du volcanisme Tertiaire de 1'Iran Central. [Dissertation], Grenoble, 489 pp. (1981).
11. Harris N.B.W., Pearce J.A., and Tindle A.G. Geochemical characteristics of collision zone magmatism. In: Coward M.P. and Rise A.C. (Eds.), Collision tectonics. *Geol. Soc. Spec. Publ.*, **19**: 67-81 (1986).
12. Hassanzadeh J. Metalogenic and tectonomagmatic event in the SE sector of Cenozoic active continental margin of Central Iran (Shahr-e-Babak), Kerman Province. Ph.D. thesis, California, Los Anjeles, 204 pp. (1993).
13. Ishihara S. The magnetite-series and ilmenite-series granitic rocks. *Min. Geol.*, **27**: 293-305 (1977).
14. Kuno H. Differentiation of basalt magmas. In: Hess H.H. and Poldervaart A. (Eds.), *Basalts*, 2, John Wiley and Sons, 623-688 (1968).
15. Le Maitre R.W. *A Classification of Igneous Rocks and Glossary of Terms*. (with Bateman P., Dudek A., Keller J., Lameyre J., LeBas M.J., Sabin P.A., 16-Schmid R., Sorensen H., Streckeisen A., Wooley A.R., and Zanettin B.), Blackwell, Oxford, 193 pp. (1989).
16. Maniar P.D. and Piccoli P.M. Tectonic discrimination of granitoids. *Geol. Soc. Am. Bull.*, **101**: 635-643 (1989).
17. Muller D., and Groves D.I. *Potassic Igneous and Associated Gold-Copper Mineralization*. Springer, 241 pp. (1997).
18. Nakamura N. Determination of REE, Ba, Mg, Na and K in carbonaceous and ordinary chondrites. *Geochim. Cosmochim. Acta*, **38**: 757-775 (1974).
19. Nelson S.T. and Montana A. Sieve-textured plagioclase in volcanic rocks produced by rapid decompression. *Am. Mineral.*, **77**: 1242-1249 (1992).
20. Pearce J. Sources and settings of granitic rocks. *Episodes*, **19**: 120-125 (1996).
21. Pearce J.A., Harris N.B.W., and Tindle A.G. Trace element discrimination diagrams for the tectonic interpretation of granitic rocks. *J. Petrol.*, **25**: 956- 983 (1984).
22. Pe-Piper G., Piper D.J.W., and Matarangas D. Regional implications of geochemistry and style of emplacement of Miocene I-type diorite and granite, Delos, Cyclades, Greece. *Lithos*, **60**: 47-66 (2002).
23. Schroeder J.W. Essai sur la structure de l'Iran. *Ecologae Geol. Helv.*, **37**: 37-81 (1944).
24. Sheppard S.; Occhipinti S.A., and Tyler I.M. The relationship between tectonism and composition of granitoid magmas, Yarlarweelor gneiss complex, western Australia. *Lithos*, **66**: 133-154 (2003).
25. Soesoo A. Fractional crystallization of mantle derived melts as a mechanism for some I-type granite petrogenesis; an example from Lachan folded belt, Australia. *J. Geol. Soc. London*, **157**: 135-149 (2000).
26. Waight T.E., Weaver S.D., and Muir R.J. The Hohonu Batholith of North Westland, New Zealand: granitoid compositions controlled by source $H_2O$ contents and generated during tectonic transition. *Contrib. Mineral. Petrol.*, **130**: 225-239 (1998).
27. Wilson M. *Igneous Petrogenesis: A Global Tectonic Approach*. (2nd Ed.), Harper Collins Academic, London, 466 p. (1991)
28. Zen E.-an. Aluminum enrichment in silicate melts by fractional crystallization: some mineralogic and petrographic constraints. *J. Petrol.*, **27**: 1095-1118 (1986).